# Comparison between the non orographic gravity wave drag schemes used in global climate models to simulate a quasi-biennial oscillation and constant level balloons

**F. Lott[1], R. Rani[1], C. McLandress[4], A. Podglagen[1], A. Bushell[4], M. Bramberger[4], H.-K. Lee[4], J. Anstey[4], H.-Y. Chun[4], Y.-H. Kim[4], B. Legras[1], E. Manzini[4], H. Naoe[4], S. Osprey[4], R. Plougonven[3], H. Pohlmann[4], J. Richter[4], J. Scinocca[4], J. Serrano[4], F. Serva[4], T. Stockdale[4], S. Versick[4], S. Watanabe[4], K. Yoshida[4], and... list not closed**

[1]Laboratoire de Météorologie Dynamique (LMD)/IPSL, PSL Research Institute, Ecole Normale Supérieure, Paris, France.
[2]LMD/IPSL, Sorbone Université, Paris, France.
[3]LMD/IPSL, Ecole Polytechnique, Institut Polytechnique de Paris, Palaiseau, France
[4]**Provide your affiliation please, shorter is better**

**Key Points:**

- Temptative, but somethink like:
- The non-orographic parameterization tuned to produce a realistic tropical quasi-biennial oscillation in global climate models are used to predict in-situ observations.
- Parameterized gravity waves needed in large-scale models have realistic amplitudes in the tropical lower stratosphere.
- Day-to-day variations of the estimated gravity wave momentum fluxes correlate in some cases with observations, except when launching level are near the tropopause.
- The probability density distribution of the parameterized momentum fluxes are better reproduced when the schemes are not related to their convective sources and/or the launching level in the lower and middle troposphere.

**Version 0, date: October 31, 2023**

Corresponding author: Francois Lott, `flott@lmd.ens.fr`

## Abstract

Gravity Waves (GWs) parameterization schemes in 14 General Circulation Models (GCMs) participating to the Quasi-Biennial Oscillation initiative (QBOi) are directly compared to Strateole-2 balloon observations made in the lower tropical stratosphere from November 2019 to February 2020 (phase 1) and from October 2021 and January 2022 (phase 2). The parameterizations used span the 3 state of the arts techniques used in GCMs to represent subgrid scale non-orographic GWs, the two globally spectral techniques developet by (Hines, 1997) and (Warner & McIntyre, 1999) respectively and the "multiwaves" approaches following (Lindzen, 1981). The input meteorological fields necessary to run the parameterizations offline are extracted from the ERA5 reanalysis and correspond to the instantaneous meteorological conditions found underneath the balloons. In general, the amplitudes are in fair agreement between measurements of the momentum fluxes due to waves with periods less than 1 hr and the parameterizations. The correlation of the daily values between the observations and the results of the parameterization can be around 0.4, which is statistically elevated considering that we analyse around 1200 days of data and sometime good considering that the parameterizations have not been tuned: the schemes used are just the standard ones that help producing a Quasi-Biennial Oscillation in the corresponding model. These correlations nevertheless vary considerably between schemes and depend little on their formulation (globally spectral versue multiwaves for instance). We therefore attribute it to dynamical filtering all schemes taking good care of it, whereas only few relate the gravity waves to their sources. Except for one model, significant correlations are mostly gound for eastwrd propapgating waves, which may be due ti the fact that during both Strateolo 2 phases the QBO phase is eastely at the altitude of the balloon flights. On the other hand, statistical properties, like pdf of momentum fluxes seem better represented in spectral schemes with constant sources than in schemes ("spectral" or "multiwaves") that relate GWs to their convective sources.



## Plain Language Summary

In most large-scale atmospheric models, gravity wave parameterizations are based on well understood but simplified theories and parameters which are keyed to reduce systematic errors on the planetary scale winds. In the equatorial regions, the most challenging errors concern the Quasi Biennial Oscillation. Although it has never been verified directly, it is expected that the parameterizations tuned this way should transport a realistic amount of momentum flux in both the eastward and westward directions when compared to direct observations. Here we show that it is the case, to a certain extent, using constant-level balloon observations at 20 km altitude. The method consists in comparing directly, each day and at the location of the balloon the measured momentum fluxes and the estimations from the gravity wave parameterizations used in the global models that participate to the Quasi-Biennal Oscillation intiative and when using observed values of the large-scale meteorological conditions of wind, temperature, precipitation, and diabatic heating.

# 1 Introduction

It is well known that the large scale circulation in the middle atmosphere is in good part driven by gravity waves (GWs) that propagate in the stratosphere (Andrews et al., 1987). These waves carry horizontal momentum vertically and interact with the large scale flow when they break. The horizontal scale of these waves can be quite short, much shorter than the horizontal scale of General Circulation Models (GCMs) so they need to be parameterized (Alexander & Dunkerton, 1999). In the tropics, the convective GWs are believed to dominate largely (Fovell et al., 1992; Alexander et al., 2000; Lane & Moncrieff, 2008), they contribute significantly to the forcing of the Quasi-Biennial Oscillation (QBO), a near 28-month oscillation of the zonal mean zonal winds that occurs in the lower part of the equatorial stratosphere (Baldwin et al., 2001). For these reasons, the parameterization of convective GWs is necessary for most GCMs to explicitly realize the QBO.

Although gravity wave parameterizations are now used in many models with success including in the tropics (Anstey et al., 2016; Scinocca, 2003; Orr et al., 2010; Christiansen et al., 2016) (Serva et al., 2018)(Beres et al., 2005; Song & Chun, 2005; Lott & Guez, 2013; Bushell et al., 2015), their validation using direct in situ observations remains a challenge. There exist observations of GWs using global satellite observations (Geller et al., 2013) but the GWs identified this way still have quite large horizontal scales, and some important quantities like the Momentum Fluxes (MFs) are often deduced indirectly, for instance from temperature measurements using polarization relations (Alexander et al., 2010; Ern et al., 2014). For these two reasons, in situ observations are essential, and the most precise ones are provided by constant-level long-duration balloons, like those made in the Antarctic region during Strateole-Vorcore (Hertzog, 2007) and Concordiasi (Rabier et al., 2010), or in the deep tropics during PreConcordiasi (Jewtoukoff et al., 2013) and more recently Strateole 2 (Haase et al., 2018). Among many important results, these balloon observations have shown that the momentum flux entering in the stratosphere is extremely intermittent (Hertzog et al., 2012). This intermittency implies that the mean momentum flux is mostly transported by few large-amplitude waves that potentially break at lower altitudes than when the GW field is more uniform. This property, when reproduced by a parameterization (de la Cámara et al., 2014; Kang et al., 2017; Alexander et al., 2021), can help reduce systematic errors in the midlatitudes, for instance on the timing of the final warming in the Southern Hemisphere polar stratosphere (de la Cámara et al., 2016), or on the QBO (Lott, Guez, & Maury, 2012). Balloon observations have also been used to characterize the dynamical filtering by the large scale winds (Plougonven et al., 2017), and to validate the average statistical properties of the GW momentum flux predicted offline using reanalysis data (Kang et al., 2017; Alexander et al., 2021). However, the evaluation of parameterizations using balloon observations have have often been quite indirect so far, with the common belief that the best a parameterization can do is to reproduce a realistic statistical behaviour (Jewtoukoff et al., 2015; Kang et al., 2017; Alexander et al., 2021). and there are few good reasons for that. For example, parameterizations are often based on simplified quasi-linear wave theory, they assume spectral distributions that are loosely constrained, and they ignore lateral propagation almost entirely (some attempt to include it can be found in Amemiya and Sato (2016)). Nevertheless, some factors could mitigate these weaknesses. One is that in most parameterizations the wave amplitude is systematically limited by a breaking criterion that encapsulates nonlinear effects. An other is that some parameterizations explicitly relate launched waves to sources, and there is constant effort to improve the realism of the convective ones (Liu et al., 2022). Also, observations systematically suggest that dynamical filtering by the large scale wind is extremely strong for upward propagating GWs (Plougonven et al., 2017), and this central property is represented in most GW parameterizations. For all these reasons, it may well be that GW parameterizations keyed to the large scale conditions found at a given place and time gives MFs that can be directly compared to the MFs measured by a balloon at the same place.

Based on the relative success of the offline calculations done in the past using reanalysis data (Jewtoukoff et al., 2015; Kang et al., 2017; Alexander et al., 2021), (Lott et al., 2023) have shown that such a direct comparison gives result of interest. The first is that a state of the art convective gravity wave drag scheme, predicts momentum fluxes in the low equatorial stratosphere which amplitude can be directly compared with those measured during the Strateole-2 balloon flights. It gives a direct in-situ observational confirmation that the theories and modelling of the QBOs developed over the last 50 years were in good part correct about the significance of the GWs to the QBO forcing. Also interesting, the comparison showed a good level of correlation between the day to day variability in momentum fluxes between measured and observed fluxes, a correlation that is much better for waves carrying momentum fluxes in the eastward direction than in the westward direction. It was suggested that such a good ccorrelation was due to the fact that the (Lott & Guez, 2013) scheme analysed relate the gravity waves to their convective sources (not all schemes do) and that the GWs experience significant dynamical filtering in the middle troposphere and lower stratosphere. (Lott et al., 2023) nevertheless revealed that a scheme that relates gravity waves to convection only somehow failed in predicting the right statistical behaviour of the momentum fluxes, the pdfs showing a long tail for low values of the MFs, suggeting missing processes like lateral propagation or the presence of a background of waves which origin remains a challenge to predict.

The purpose of this paper is to continue such a direct comparison using the most recent observations and near all the gravity wave parameterization schemes used by the modelling groups participating to the Quasi-Biennial Oscillation initiative (QBOi, (Butchart et al., 2018)). We will follow for that (Lott et al., 2023) and use the 8 balloons of the first phase of the Strateole 2 campaign that flew in the lower tropical stratosphere between November 2019 and February 2020 and extent it to the 15 balloons that flew more than one day during the second phase of the Strateole 2 campaign, between October 2021 and January 2022. For each of the flights and each time, we have identified the grid point in the ERA5 reanalysis (Hersbach et al., 2020) that is the nearest and used the vertical profiles of wind and temperature as well as the surface value of precipitation to emulate the parameterization of GWs used in the global models that participated to the Quasi-Biennial Oscillation initiative (QBOi). We also extract from the analysis and short range forecast, diabatic heatings and the cloud base and top altitudes needed in some schemes to predict gravity waves.

## 2 Data and method

### 2.1 Parameterizations of non orographic gravity wave schemes

The parameterizations schemes used to predict orographic gravity waves belongs to two well separated families, dating back from the 1980's when it becomes evident that a goood simulation of the middle atmosphere by global atmospheric models could not be done without taking into account non-orographic gravity waves. The first family roots in the formulation by (Lindzen, 1981), where the gravity wave field field is represented by gravity waves monochromatic in the horizontal space and time. It was extended to treat a large ensemble of waves by (Alexander & Dunkerton, 1999) making the asumption that the breaking of each waves could be made independent from the others. An advantage of such schemes is that it roots in linear theories where sources like convection and/or fronts can be introduced using closed form theories (Beres et al., 2005; Song & Chun, 2005; Richter et al., 2010; Lott & Guez, 2013; de la Cámara & Lott, 2015). In the following we will refer to such schemes as "multiwave", they are expensive because they request a large amount of waves to represent well a realistic wave field, but this limit can easily be circumvented by using stochastic approaches (Eckermann, 2011; Lott, Plougonven, & Vanneste, 2012). As an alternative, but also to better represent breaking, many centers developed globally spectral schemes. These schemes uses the observationnal fact that

| | $p_l$ | $F_{LT}$ | $2\pi/m_*$ | $C_{\rm min}$ |
|---|---|---|---|---|
| CMAM | 100hPa | 1.3mPa | 1km | 0.25 m/s |
| IFS | 450hPa | 5mPa | 3km | 0.5 m/s |
| ECEarth | 450hPa | 3.75mPa | 2km | 0.25 m/s |
| UKMO | 1000hPa | Precip | 4.3km | ? |

**Table 1.** WMI Parameters changing between CMAM, IFS, ECEarth, and UKMO. UKMO is shown distinctly because it is based on (Warner & McIntyre, 1999) simplified version of WMI rather than on (Scinocca, 2003)'s and realte launched MF to precipitations.

in observations the vertical shape of the spectra have a quite universal character. In the early 1990's (Hines, 1991) developed a theory where GW breaking is represented by imposing an upper limit to the range of vertical wavenumber, the limit being calculated according to the large scale wind and including a Doppler spreading by the other gravity waves (see also (Hines, 1997)). The scheme has been implemented with success in various GCMs (see for instance (Manzini et al., 1997)), and will be referred to as "HDS" in the following. As an alternative, the theory in (Warner & McIntyre, 1996) imposes gravity wave saturation according to an empirical spectra but treat vertical changes in the spectra following GWs propagation invariant character. The theory has been simplified and/or optimized to permit implementation, for instance in the UKMO model (Warner & McIntyre, 1999; Scaife et al., 2002) and in the CMAM model (Scinocca, 2003) respectively, and will be refered to has "WMI" in the following. To a certain extent, the spectral schemes can also take into account the relation with sources, for instance the HDS scheme has been related to fronts in (Charron & Manzini, 2002), and the UKMO version of the WMI scheme to precipitations in (Bushell et al., 2015).

In the present paper, we are going to compare the GWs schemes used in 14 of the models that participate to QBOi, all belonging to one of the three type of schemes described above (WMI, HDS, and Multiwave), all the multiwave schemes relating GWs to their convective sources, only one of the spectral scheme doing so, the UKMOgws WMI scheme in (Bushell et al., 2015), its results will be discussed with the source-related multiwave scheme.

Among the 14 models, three use the (Scinocca, 2003)'s version of the WMI: CMAM, IFS and ECEarth. Their version for QBOi and further detailed in (Anstey et al., 2016; Orr et al., 2010; Davini et al., 2017), they essentially differ by four parameters, the launch level pressure $p_l$, the launched momentum flux $F_{LT}$, the characteristic vertical wavenumber $m_*$ and a minimum intrinsic phase speed in the launched spectra Note that for EC-Earth the exact value of the parameters are from J. Garcia Serrano (private communication).

Still among the 14 models, 5 uses the (Hines, 1997)'s parameterization schemes presented in (Manzini et al., 1997). Between the five models, and in the Hines scheme, only changes between models the launching level $p_l$, the root mean square of the horizontal wind variability due to GWs at launch level $\sigma$, as well as an effective horizontal wavenumber $K^*$. There are also more numerical parameters that eventually changes, a minimum value for the the cutoff vertical wavenumber $m_{\rm min}$, and two parameters that control smoothing in the vertical of the GWs root mean square variance and cut-off vertical wavenumber, the coefficient $C_{\rm smo}$ and the number of time the smoothing is applied $N_{\rm smo}$.

| | $p_l$ | $\sigma_s$ | $2\pi/K^*$ | $m_{\text{min}}$ | $C_{\text{smo}}$ | $N_{\text{smo}}$ |
|---|---|---|---|---|---|---|
| ECham5 | 450hPa | 1. | 125km | 0 | 2 | 5 |
| MIROC | 650hPa | 0.95 | 250km | $6.5\ 10^{-5}$ | 2 | 2 |
| MPIM | 650hPa | 1.2 | 125km | 0 | 2 | 2 |
| MRI-ESM | 700hPa | 1.9 | 1250km | $3.3\ 10^{-4}$ | 4 | 2 |
| EMAC | 650hPa | 1. | 125km | 0 | 2 | 2 |

**Table 2.** HDS Parameters changing between ECHam5, MIROC, MPIM, MRI-ESM, and EMAC.

| | $p_l$ | Phase Speed | $\Delta z$ | Source |
|---|---|---|---|---|
| LMDz | 500hPa | -30m/s<Intrinsic<30m/s | 1km | Precip |
| Yonsei | 900hPa-100hPa | -100m/s<Absolute<100m/s | 100m-15km | Heating rate |
| WACCM | ? | | | Heating rate |

**Table 3.** Some parameters changing between LMDz, YONSEI and WACCM, for information only the schemes being extremely distinct

Finally the last 4 schemes we consider all links GWs to sources (convection or precipitation), 3 are multiwaves and have been developed independently one from the others, LMDz, YONSEI, and WACCM and 1 uses the ultra simple version of the WMI schemes presented in (Warner & McIntyre, 1999; Bushell et al., 2015) rather than the (Scinocca, 2003)'s version. The differences between these schemes are numerous it is impossible to details them, the reader is referred to the corresponding papers. The most salient differences are in the source term. In LMDz is made the choice to relate the launched MF to square precipitation $P_r^2$ consistent with linear theory before breaking (Lott & Guez, 2013) whereas in (Bushell et al., 2015) it is related to $\sqrt{P_r}$. In the Yonsei's scheme (Song & Chun, 2005; Choi & Chun, 2011), the launched momentum flux is directly related to convective heating distributed in the vertical between the cloud bottom and cloud top, the launch altitude being at the cloud top. In this case the launching level can vary between $2km$ and 15km typically and the depth of the heating between 100m and $15km$. Also, the absolute phase speed cover the ranges 100m/s $< C_{abs} <$ 100m/s.

### 2.2 Offline parameterization runs

To activate the schemes in offline mode we will use ERA-5 hourly data of precipitation and 3-hourly data of winds, surface pressure, temperature, cloud liquid and ice water content at $1^o\times1^o$ horizontal grid to mimic a large scale climate model resolution. Winds, surface pressure, temperature, and water contents are then linearly interpolated on 1hr time step to be synchronised with precipitation. In the vertical we use data at 67 model levels, taking one every two ERA5 levels, to speed up calculations. To estimate convective heating rates vertical profiles, we follow (Fueglistaler et al., 2009) and evaluate diabatic heating using ERA5 hourly data from short range forecast and as a residual between the parameterized temperature tendency and the radiative heatings (longwave plus shortwave). When needed, we also evaluate the cloud bottom height and top height using the cloud water content (liquid+ice) from ERA5 reanalysis.

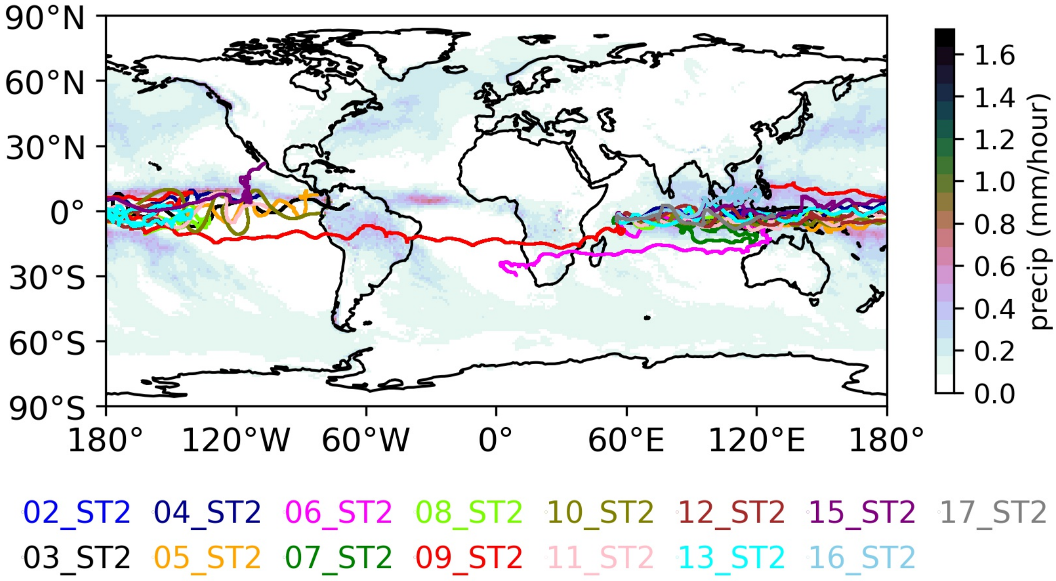


**Figure 1.** Strateole 2, Phase 2 balloon trajectories taking place between October 2021 and January 2022. Shading presents the precipitation field from ERA5 averaged over the period.

### 2.3 Strateole 2 balloon observations

The in situ observations we use are from the 8 balloons of the first phase of the Strateole 2 campaign that flew in the lower tropical stratosphere between November 2019 and February 2020 and from the 15 balloons that flew more than one day during the second phase of the Strateole 2 campaign, between October 2021 and January 2022. The trajectories during phase 2 are shown in Figure 1, superimposed upon the averaged precipitation (the same Figure but fir phase 1 is in (Lott et al., 2023)). In the MFs calculated from observations Corcos et al. (2021) distinguish the waves with short periods (1hr-15mn) from the waves with period up to one day (1d-15mn). They also distinguish the eastward waves giving positive MF in the zonal direction from the westward waves giving negative MF. As shows Fig. **??**, it is coincidental that the phase 1 flights took place during the 2nd documented QBO disruption (Anstey et al., 2021), but the fact that the measurements are below the altitude at which the disruption manifests makes us believe that our comparison between gravity wave MFs over the period is not much affected by the disruption (beyond the fact that the disruption potentially affects the large scale winds, which is something that translates well in the parameterization). It is also important to notice that during phase 2, the large scale winds conditions in the lower stratosphere are almost as during phase one at balloons altitudes (end of eastward QBO phase).

In the following we will compare the momentum fluxes derived from the balloon data, emphasize the intrinsic frequencies that the scheme represents (the intrinsic periods below $1hr$) and consider the ERA5 data at the points that are the nearest from the balloon. The prediction is then made every hour and averaged over the day, again because this is the time scale needed for our scheme to sample realistically a GW field, and also because it takes around a day for a balloon flight to cover about a model gridscale. We will discuss sensitivities to these choices in the first paragraph of the conclusion.

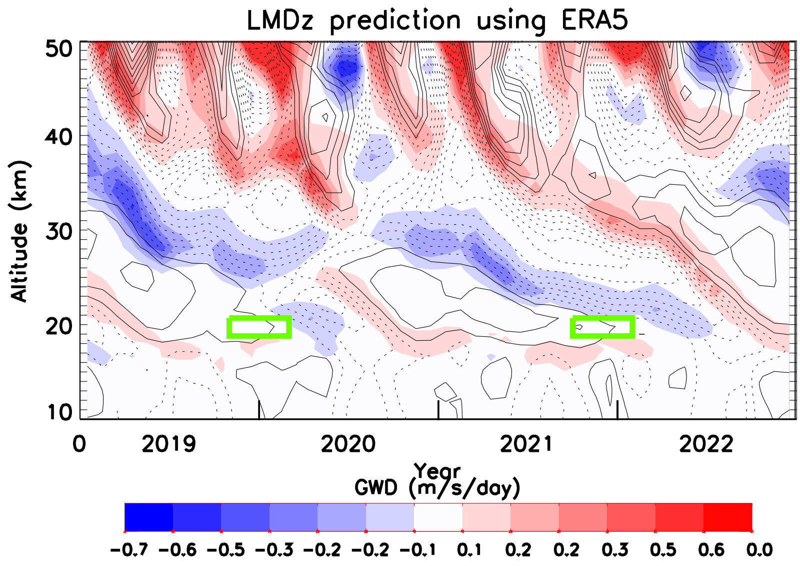


**Figure 2.** Time vertical sections of the zonal mean zonal wind (CI=10m/s, negative values are dashed and non-orographic gravity wave tendency averaged over the Equatorial band ($-6S \quad - \quad +6N$). Input data are from ERA5 reanalysis and GWs prediction from the LMDz scheme. The 2 green boxes indicate schematically the altitude and time ranges of the Strateole 2 phase 1 and 2 flights considered in this study.

## 3 Results

**THIS SECTION IS UNDER PROGRESS, ONLY THE FIGURES SHOULD BE CONSULTED**

Figure 3 shows time series of daily values of momentum fluxes predicted by the parameterizations and measured during balloon flights 2 from strateole 2 phase 1. This is also the flight shown in Fig. 3 in (Lott et al., 2023), and where was also shown the time series of daily precipitation and zonal wind at flight altitude. The top panel is for the WMI based schemes, the middle panel for the HDS schemes and the bottom panels for the schemes relating the GWs fluxes to their sources. In all panels the black curves are for the daily observations. For clarity we present results for the Eastward and westward MF only. Overall ones sees that the schemes predict momentum flux values that somehow compare with the observed one, at least in terms of amplitude. In the globally spectral schemes (upper and middle panels), we also see that the parameterizations predict peaks in MF which duration and amplitudes looks reasonnable compared to the observed ones. More specifically, and in the eastward direction there are pronounced peaks after day sixty, peaks that (Lott et al., 2023) related to the fact that after this date the zonal wind at balloon altitude is westward a situation that favors eastward waves. Of course in terms of amplitude there are varibilities between the models schemes, but the qualitative behaviours look reasonnable. There is nevertheless one exception, the CMAM scheme predicts long lasting plateau, maybe for this scheme the fact that the launching altitde is quite high, mitigate the dynamical filtering between the launching level and the balloon flight.

The fact that the parameterizations estimates fluxes of about the right amplitude is summarized in Figure 5, where the average of the fluxes over all strateole flights that last than a month (18 flight in total) are shown. It confirms systematically that the offline estimations are quite good on average and in the zonal direction, for the eastward

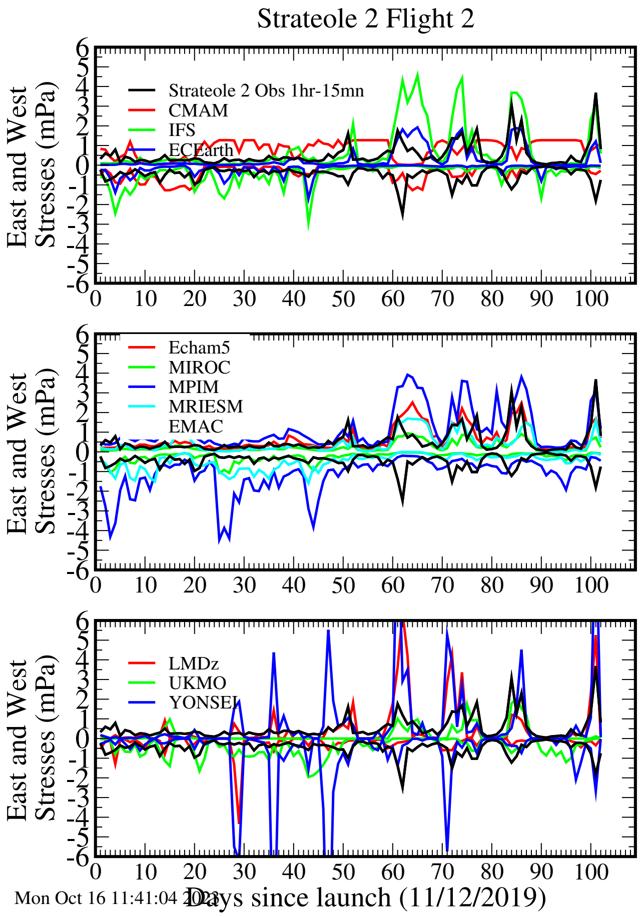


**Figure 3.** Comparison between daily averaged values of the eastward and westward MFs measured by the balloons during Strateole 2 Flight 1 and estimated by the GW schemes at the balloon location and altitude. Colored curves are for the GW schemes predictions using ERA5 and from different models, black curves are for the observed MFs due to the 15mn-1hr GWs.

and westward components again. The Figure 6 group the models averaging the eastward and westward fluxes over all the balloon flights, confirming again that the parameterizations used fall around the observed values. There is varibilities between the models, but there is no tendency for the models to vcollectively need much more or much less gravity wave stress than needed.

The curves in Figure 3 and Figure 4 also suggest that observations and offline estimations evolve quite similarly day after day, both measured and parameterized MFs being sensitive to precipitation and dynamical filtering. To test more systematically this relationship, we also calculated the correlations between measured and estimated MFs and for each flight (Table **??**). To test the significance, we measure the number of Degrees of Freedom (DoF) present in each dataset, and calculate for that the decorrelation time scale, which we take as the lag in day beyond which the lag-autocorrelation of the series falls below 0.2. As this time-lag varies from one series to the other, we give explicitly in column 5, the number of DoF, which is the duration of the flight divided by the decorrelation time scale. Note that for their decorrelation time, we consider for simplicity that evaluated with daily averaged observations, but found that it is not much different from that evaluated with the offline estimates (not shown). In each case, we find

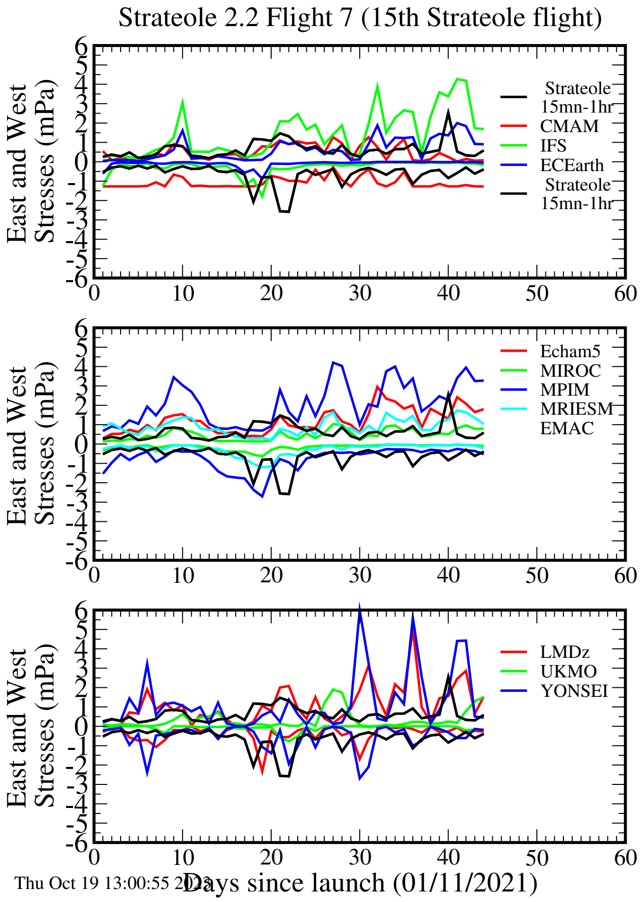


**Figure 4.** a) Same as Fig 3 but for Strateole 2 Phase 2 Flight 7.

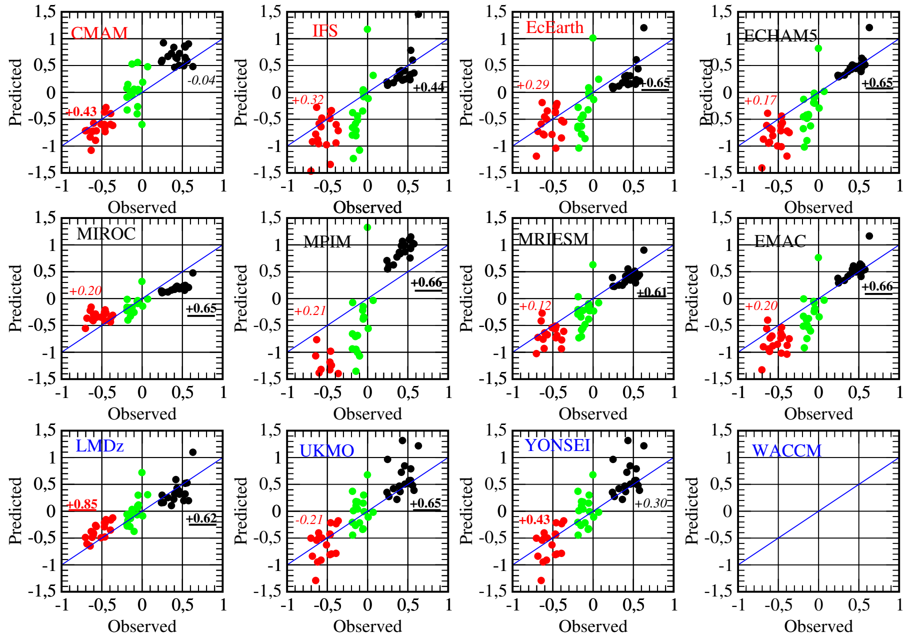


**Figure 5.** Scatter plot of the momentum fluxes measured by the balloon versus parameterized using different models. Only considered here the 18 balloon flights that last more than a month (East: black; West: red; Cumulated: green). Also shown are the correlations between observations and predictions, 99% significant levels are bold underlined, 95% are bold. Non significant values are shown in italic for information. The number of DoF for Pearson test is 18, about the number of balloon flights that last more than a month.

positive correlations, they are often significant in the Eastward direction the estimated westward being much more difficult to predict. In the eastward directions, differences seems more related to the launching altitude than to the nature of the scheme, CMAM lauching waves near the tropopause whereas YONSEI often does so when clouds extent over the entire troposphere, in which case little dynamical filtering can occur between the launching level and the quite nearby flights.

A major differences between the scheme, is that in some the GW activity is related to convective heating or precipitation, whereas others consider uniform sources. In the first case its means that momentum fluxes could be underestimated in many circumstances, despite the fact that the amplitudes are realistic when considering long term averages. To analyse better this difference and its potential consequences, the Figure **??** presents PDFs of the distributions of the momentum fluxes considering all the daily data. For the PDFs (solid line), one sees that the balloons almost systematically measure fluxes with amplitude between 0.1mPa and 10mPa (see Figure **??**a), whereas in the parameterizations with convective/precipitation sources there are many more contributions from the smaller amplitude momentum fluxes (solid red), not mentioning that the zero values are excluded from PDFs when plotted versus the logarithm of MF amplitudes.

## 4 Conclusion

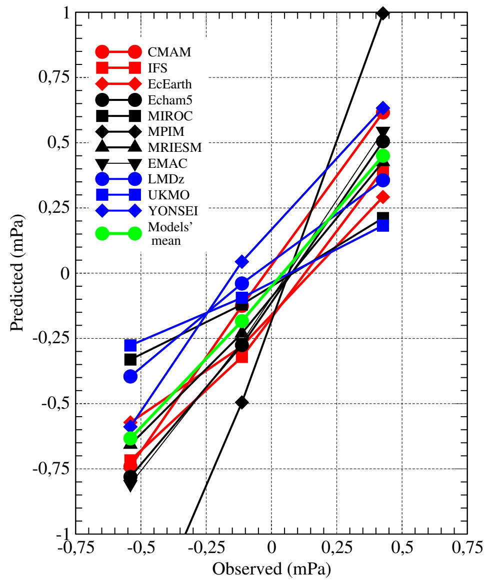


**Figure 6.** East, West and cumulated zonal momentum fluxes averaged over the Strateole 2 phase 1 and 2 period period and according to participating models.

| East | Day Dof | CM AM | IFS | ECE ARTH | Ech am5 | MI ROC | MPI M | MRI ESM | EM AC | LMD z | UK MO | YON SEI |
|---|---|---|---|---|---|---|---|---|---|---|---|---|
| Phase 1 | 670-216 | -0.07 | 0.53 | 0.52 | 0.52 | 0.48 | 0.49 | 0.44 | 0.48 | 0.49 | 0.34 | 0.32 |
| Phase 2 | 621-322 | -0.19 | 0.41 | 0.38 | 0.38 | 0.33 | 0.34 | 0.30 | 0.33 | 0.40 | 0.34 | 0.20 |
| Phase 1+2 | 1291-538 | -0.11 | 0.49 | 0.47 | 0.45 | 0.41 | 0.41 | 0.36 | 0.40 | 0.46 | 0.34 | 0.27 |
| West | Day Dof | CM AM | IFS | ECE ARTH | Ech am5 | MI ROC | MPI M | MRI ESM | EM AC | LMD z | UK MO | YON SEI |
| Phase 1 | 670-216 | 0.14 | -0.07 | -0.07 | -0.13 | -0.03 | -0.04 | -0.04 | -0.04 | 0.30 | -0.03 | 0.10 |
| Phase 2 | 621-322 | 0.21 | 0.18 | 0.16 | 0.03 | 0.00 | 0.01 | 0.05 | -0.01 | 0.40 | 0.04 | 0.13 |
| Phase 1+2 | 1291-538 | 0.17 | 0.05 | 0.04 | -0.05 | -0.02 | -0.02 | 0.01 | -0.02 | 0.34 | 0.00 | 0.11 |

**Table 4.** Correlation between observed and measured fluxes, strateole phases 1 and 2.

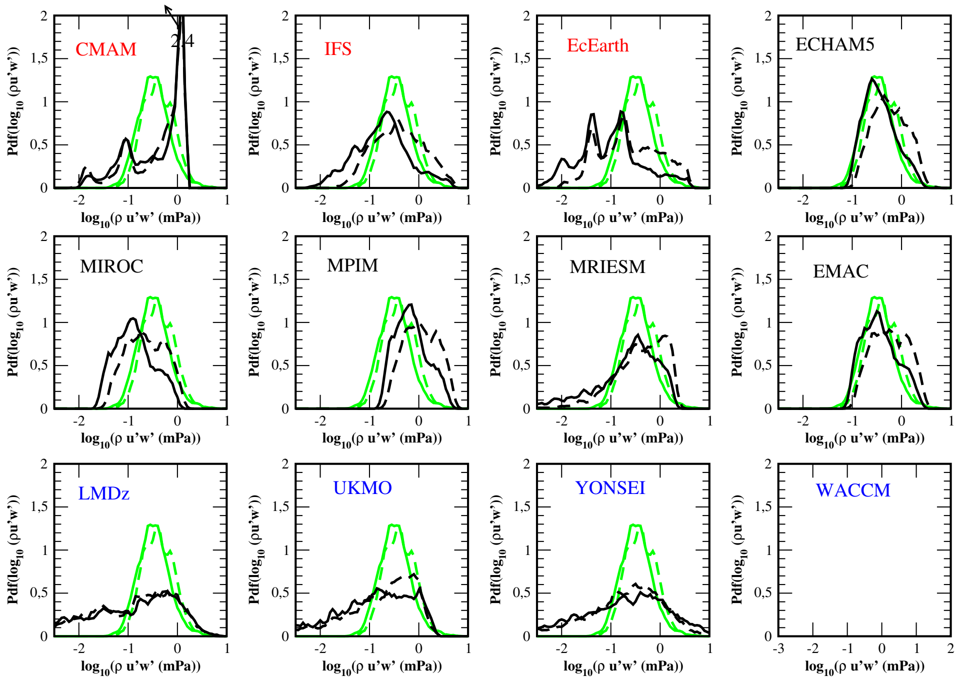


**Figure 7.** PDFs of daily values of Momentum flux distribution. The PDFs are calculated from histograms of 1291 MFs daily value within intervals of $\Delta\left(\log_{10}\rho\overline{u'w'}(\text{mPa})\right) = 0.05$, thereafter smoothed by a 5 point non-recursive filter with weight $(0.1, 0.2, 0.4, 0.2, 0.1)$. Measured values are in green, estimations using ERA5 data and the parameterizations are in black. Solid lines are for Eastward, dashed lines are for Westward.

## 5 Open Research

Balloon data presented in (Haase et al., 2018) can be extracted from the STRATEOLE 2 dedicated web site: https://webstr2.ipsl.polytechnique.fr

ERA5 reanalysis data are described in (Hersbach et al., 2020) and can be extracted from the COPERNICUS access hub: https://scihub.copernicus.eu/

The LMDz-6A GCM used for CMIP6 project is described in (Hourdin et al., 2020), it can be directly installed from the dedicated webpage: https://lmdz.lmd.jussieu.fr/utilisateurs/installation-lmdz

## Acknowledgments

This work was supported by the VESRI Schmidt Future project "DataWave".

## Appendix: Running the offline code

To run the models parameterizations in offline mode and compare with daily values of momentum fluxes measured during strateole 2, download the file offline_v9_Strateole_QBOi_Open.tar, on the web page:

wget `https://web.lmd.jussieu.fr/~flott/DATA/offline_v9_Strateole_QBOi_Open.tar.gz`

Then gunzip and do tar -xvf offline_v9_Strateole_QBOi_Open.tar

In the directory, offline_v9_Strateole_QBOi_Open:

Run directory It basically contains a script that compile the programs, link to the input dataset and produce various outputs. The Makefile certainly needs to be adapted to the computer.
To launch predictions for Strateole-2 phase 1, launch: ./laun_ph1ball_gwd_era5.sh
For phase 2, ph1→ph2.

Fortran Codes: all the fortran routines are located in prog.
**laun_gwd_era5.f90:** Main program loading input data in netcdf format and calculating drag and momentum fluxes at the balloon place.
**preci_gwd_LMDz_QBOi.f90:** LMDz Multiwaves routines predicting gwdrag from precipitation
**gwsat_Modnam.f90:** the globally spectral scheme using the (Warner & McIntyre, 1996)'s scheme version by J. Scinocca.
**hinesgw6g_plus_subs.f** HDS scheme
**gw_ussp_core.f90:** The WMI scheme with amplitude keyed to precipitation used in some UKMO runs.
**cgwcalc.f90:** Multiwave scheme developped at Yonsei's university

Input Data: All the input data are located in the directories hourly_ph1 and hourly_ph2 for phase 1 and 2 respectively. For instance, 1hr average of the strateole2 momentum fluxes are in
ALL_STRATEOLE2_Balloon_ph1_1day15min.nc
and
All_STRATEOLE2_Balloon_ph1_1hrs15min.nc
for the waves with periods between 1day and 15mn and between 1Hr and 15 mn respectively.
Still in this directory, the ERA5 reanalysis products, which include winds temperature, cloud liquid water, and surface log pressure, over a 5°x5° domain centered at the balloons drifting locations are in Input_ERA5_data_all_variables_balloons_ph1.nc.
Precipitation every hours are also included. The diabatic heatings are from fore-

cast. All datas that are only provided every 3hr are linearly interpolated in time to give hourly values.

Output data (Part 1)

All the ouputs are in the output_ph1 and output_ph2 directories:

**Netcdf**: contains the output of the schemes in netcdf format on the vertical column and over the 5°x5° domain over which the ER5 data are provided. There is one netcdf dataset by balloons flight each contains output from all the schemes.

**Balloon_alt** After post processing by the python scripts launch_script_obs.py, are extracted the MFs at balloon flight altitude.

Python Scripts

A serie of Python scripts, located into python_script are proposed to compare the outputs of the scheme to the balloon data.

**launch_script_obs.py**: Reads the balloon flight data of MFs and averaged over 1day and writte them in text format ( ending with '.dat') and stored in **output/Balloon_alt/obs_output**

**launch_prediction_eachB_ysei.py**: extract from the prediction the values of the MFs at the balloons place and altitude. Results stored in text format (".dat" in **Balloon_alt/Pred_output_Balloon_altitude/**.

The next python scripts are cosmetic in the sense that they use the above two datasets to make plots of timeseries balloon averaged values, evaluate correlations, and histograms.

**timeseries_obs_pred_plot_all.py** Produces a lot of time series for each model and flights.

Output data (Part2) As a result, you can visualize timeseries of each flight here:

**output**_*ph*1**/Balloon_alt/figure_timeseries**

Histograms here: **output_ph1/histo**

Scatter plots and correlations here **output_ph1/correlation**

For phase 2, change ph1 in ph2.

xmgrace Alternative to calculate these diagnostics using fortran programs and xmgrace, the programs permit to combine statistics over the 2 phases of Strateole2.

## References

Alexander, M. J., Beres, J. H., & Pfister, L. (2000). Tropical stratospheric gravity wave activity and relationships to clouds. *Journal of Geophysical Research: Atmospheres*, *105*(D17), 22299-22309. doi: https://doi.org/10.1029/2000JD900326

Alexander, M. J., & Dunkerton, T. J. (1999). A Spectral Parameterization of Mean-Flow Forcing due to Breaking Gravity Waves. *J. Atmos. Sci.*, *56*(24), 4167–4182. doi: 10.1175/1520-0469(1999)056⟨4167:ASPOMF⟩2.0.CO;2

Alexander, M. J., Geller, M., McLandress, C., Polavarapu, S., Preusse, P., Sassi, F., … Watanabe, S. (2010). Recent developments in gravity-wave effects in climate models and the global distribution of gravity-wave momentum flux from observations and models. *Q. J. R. Meteorol. Soc.*, *136*, 1103-1124. doi: https://doi.org/10.1002/qj.637

Alexander, M. J., Liu, C. C., Bacmeister, J., Bramberger, M., Hertzog, A., & Richter, J. H. (2021). Observational validation of parameterized gravity waves from tropical convection in the whole atmosphere community climate model. *Journal of Geophysical Research: Atmospheres*, *126*(7), e2020JD033954. (e2020JD033954 2020JD033954) doi: https://doi.org/10.1029/2020JD033954

Amemiya, A., & Sato, K. (2016). A new gravity wave parameterization including three-dimensional propagation. *Journal of the Meteorological Society of Japan. Ser. II*, *94*(3), 237-256. doi: 10.2151/jmsj.2016-013

Andrews, F. G., Holton, J., & Leovy, C. (1987). *Middle atmosphere dynamics.* Academic Press.

Anstey, J. A., Banyard, T. P., Butchart, N., Coy, L., Newman, P. A., Osprey, S., & Wright, C. J. (2021). Prospect of increased disruption to the QBO in a changing climate. *Geophysical Research Letters*, *48*(15), e2021GL093058. doi: https://doi.org/10.1029/2021GL093058

Anstey, J. A., Scinocca, J. F., & Keller, M. (2016). Simulating the qbo in an atmospheric general circulation model: Sensitivity to resolved and parameterized forcing. *Journal of the Atmospheric Sciences*, *73*(4), 1649 - 1665. doi: https://doi.org/10.1175/JAS-D-15-0099.1

Baldwin, M. P., Gray, L. J., Dunkerton, T. J., Hamilton, K., Haynes, P. H., Randel, W. J., … Takahashi, M. (2001). The quasi-biennial oscillation. *Rev. Geophys.*, *39*(2), 179-229. doi: 10.1029/1999RG00007

Beres, J. H., Garcia, R. R., Boville, B. A., & Sassi, F. (2005). Implementation of a gravity wave source spectrum parameterization dependent on the properties of convection in the whole atmosphere community climate model (waccm). *Journal of Geophysical Research: Atmospheres*, *110*(D10). doi: https://doi.org/10.1029/2004JD005504

Bushell, A. C., Butchart, N., Derbyshire, S. H., Jackson, D. R., Shutts, G. J., Vosper, S. B., & Webster, S. (2015). Parameterized gravity wave momentum fluxes from sources related to convection and large-scale precipitation processes in a global atmosphere model. *Journal of the Atmospheric Sciences*, *72*(11), 4349–4371. doi: https://doi.org/10.1175/JAS-D-15-0022.1

Butchart, N., Anstey, J. A., Hamilton, K., Osprey, S., McLandress, C., Bushell, A. C., … Yukimoto, S. (2018). Overview of experiment design and comparison of models participating in phase 1 of the sparc quasi-biennial oscillation initiative ("qboi"). *Geoscientific Model Development*, *11*(3), 1009–1032. doi: 10.5194/gmd-11-1009-2018

Charron, M., & Manzini, E. (2002). Gravity waves from fronts: Parameterization and middle atmosphere response in a general circulation model. *Journal of the Atmospheric Sciences*, *59*(5), 923 - 941. doi: 10.1175/1520-0469(2002)059⟨0923:GWFFPA⟩2.0.CO;2

Choi, H.-J., & Chun, H.-Y. (2011). Momentum flux spectrum of convective gravity waves. part i: An update of a parameterization using mesoscale simulations. *Journal of the Atmospheric Sciences*, *68*(4), 739 - 759. doi: https://doi.org/10.1175/2010JAS3552.1

Christiansen, B., Yang, S., & Madsen, M. S. (2016). Do strong warm enso events control the phase of the stratospheric qbo? *Geophysical Research Letters*, *43*(19), 10,489-10,495. doi: https://doi.org/10.1002/2016GL070751

Corcos, M., Hertzog, A., Plougonven, R., & Podglajen, A. (2021). Observation of gravity waves at the tropical tropopause using superpressure balloons. *Journal of Geophysical Research: Atmospheres*, *126*(15), e2021JD035165. doi: https://doi.org/10.1029/2021JD035165

Davini, P., von Hardenberg, J., Corti, S., Christensen, H. M., Juricke, S., Subramanian, A., ... Palmer, T. N. (2017). Climate sphinx: evaluating the impact of resolution and stochastic physics parameterisations in the ec-earth global climate model. *Geoscientific Model Development*, *10*(3), 1383–1402. Retrieved from `https://gmd.copernicus.org/articles/10/1383/2017/` doi: 10.5194/gmd-10-1383-2017

de la Cámara, A., & Lott, F. (2015). A parameterization of gravity waves emitted by fronts and jets. *Geophys. Res. Lett.*, *42*(6), 2071-2078. doi: 10.1002/2015GL063298

de la Cámara, A., Lott, F., & Hertzog, A. (2014). Intermittency in a stochastic parameterization of nonorographic gravity waves. *J. Geophys. Res.: Atmospheres*, *119*(21), 11905-11919. doi: 10.1002/2014JD022002

de la Cámara, A., Lott, F., Jewtoukoff, V., Plougonven, R., & Hertzog, A. (2016). On the gravity wave forcing during the southern stratospheric final warming in LMDZ. *J. Atmos. Sci.*, *73*(8), 3213-3226. doi: https://doi.org/10.1175/JAS-D-15-0377.1

Eckermann, S. D. (2011). Explicitly Stochastic Parameterization of Nonorographic Gravity Wave Drag. *J. Atmos. Sci.*, *68*, 1749–1765. doi: 10.1175/2011JAS3684.1

Ern, M., Ploeger, F., Preusse, P., Gille, J., Gray, L. J., Kalisch, S., ... Riese, M. (2014). Interaction of gravity waves with the QBO: A satellite perspective. *Journal of Geophysical Research: Atmospheres*, *119*, 2329 - 2355. doi: https://doi.org/10.1002/2013JD020731

Fovell, R., Durran, D., & Holton, J. R. (1992). Numerical simulations of convectively generated stratospheric gravity waves. *Journal of Atmospheric Sciences*, *49*(16), 1427 - 1442. doi: 10.1175/1520-0469(1992)049⟨1427:NSOCGS⟩2.0.CO;2

Fueglistaler, S., Legras, B., Beljaars, A., Morcrette, J.-J., Simmons, A., Tompkins, A. M., & Uppala, S. (2009). The diabatic heat budget of the upper troposphere and lower/mid stratosphere in ecmwf reanalyses. *Quarterly Journal of the Royal Meteorological Society*, *135*(638), 21-37. doi: https://doi.org/10.1002/qj.361

Geller, M. A., Alexander, M. J., Love, P. T., Bacmeister, J., Ern, M., Hertzog, A., ... Zhou, T. (2013). A comparison between gravity wave momentum fluxes in observations and climate models. *J. Atmos. Sci.*, *26*(17).

Haase, J. S., Alexander, M. J., Hertzog, A., Kalnajs, L. E., Deshler, T., Davis, S. M., ... Venel, S. (2018). Around the world in 84 days [Dataset]. *Eos*, *99*. doi: https://doi.org/10.1029/2018EO091907

Hersbach, H., Bell, B., Berrisford, P., Hirahara, S., Horányi, A., Muñoz-Sabater, J., ... Thépaut, J.-N. (2020). The ERA5 global reanalysis [Dataset]. *Quarterly Journal of the Royal Meteorological Society*, *146*(730), 1999-2049. doi: https://doi.org/10.1002/qj.3803

Hertzog, A. (2007). The stratéole-vorcore long-duration balloon experiment: A personal perspective. *Space Research Today*, *169*, 43-48. Retrieved from `https://www.sciencedirect.com/science/article/pii/S1752929807800478` doi: https://doi.org/10.1016/S1752-9298(07)80047-8

Hertzog, A., Alexander, M. J., & Plougonven, R. (2012). On the Intermittency of Gravity Wave Momentum Flux in the Stratosphere. *Journal of the Atmospheric Sciences*(11), 3433–3448. doi: 10.1175/JAS-D-12-09.1

Hines, C. O. (1991). The saturation of gravity waves in the middle atmosphere. part ii: Development of doppler-spread theory. *Journal of Atmospheric Sciences*, *48*(11), 1361 - 1379. doi: https://doi.org/10.1175/1520-0469(1991)048⟨1361:TSOGWI⟩2.0.CO;2

Hines, C. O. (1997). Doppler-spread parameterization of gravity-wave momentum deposition in the middle atmosphere. part 2: Broad and quasi monochromatic spectra, and implementation. *J. Atmos. Solar Terr. Phys.*, *59*(4), 387-400. doi: 10.1016/S1364-6826(96)00080-6

Hourdin, F., Rio, C., Grandpeix, J.-Y., Madeleine, J.-B., Cheruy, F., Rochetin, N., … Ghattas, J. (2020). LMDZ6A: The atmospheric component of the ipsl climate model with improved and better tuned physics [Software]. *Journal of Advances in Modeling Earth Systems*, *12*(7), e2019MS001892. doi: https://doi.org/10.1029/2019MS001892

Jewtoukoff, V., Hertzog, A., Plougonven, R., de la Cámara, A., & Lott, F. (2015). Comparison of gravity waves in the southern hemisphere derived from balloon observations and the ecmwf analyses. *J. Atmos. Sci.*, *72*(9). doi: DOI:10.1175/JAS-D-14-0324.1

Jewtoukoff, V., Plougonven, R., & Hertzog, A. (2013). Gravity waves generated by deep tropical convection: Estimates from balloon observations and mesoscale simulations. *Journal of Geophysical Research: Atmospheres*, *118*(17), 9690-9707. doi: https://doi.org/10.1002/jgrd.50781

Kang, M.-J., Chun, H.-Y., & Kim, Y.-H. (2017). Momentum flux of convective gravity waves derived from an offline gravity wave parameterization. part i: Spatiotemporal variations at source level. *Journal of the Atmospheric Sciences*, *74*(10), 3167 - 3189. doi: 10.1175/JAS-D-17-0053.1

Lane, T. P., & Moncrieff, M. W. (2008). Stratospheric gravity waves generated by multiscale tropical convection. *J. Atmos. Sci.*, *65*, 2598–2614. doi: DOI:10.1175/2007JAS2601.1

Lindzen, R. S. (1981). Turbulence and stress owing to gravity wave and tidal breakdown. *J. Geophys. Res.*, *86*(C10), 9707-9714. doi: 10.1029/JC086iC10p09707

Liu, C., Alexander, J., Richter, J., & Bacmeister, J. (2022). Using trmm latent heat as a source to estimate convection induced gravity wave momentum flux in the lower stratosphere. *Journal of Geophysical Research: Atmospheres*, *127*(1), e2021JD035785. (e2021JD035785 2021JD035785) doi: https://doi.org/10.1029/2021JD035785

Lott, F., & Guez, L. (2013). A stochastic parameterization of the gravity waves due to convection and its impact on the equatorial stratosphere. *J. Geophys. Res.*, *118*(16), 8897-8909. doi: 10.1002/jgrd.50705

Lott, F., Guez, L., & Maury, P. (2012). A stochastic parameterization of non-orographic gravity waves: Formalism and impact on the equatorial stratosphere. *Geophys. Res. Lett.*, *39*(6), L06807. doi: 10.1029/2012GL051001

Lott, F., Plougonven, R., & Vanneste, J. (2012). Gravity waves generated by sheared three-dimensional potential vorticity anomalies. *Journal of the Atmospheric Sciences*, *69*(7), 2134-2151. doi: 10.1175/JAS-D-11-0296.1

Lott, F., Rani, R., Podglajen, A., Codron, F., Guez, L., Hertzog, A., & Plougonven, R. (2023). Direct comparison between a non-orographic gravity wave drag scheme and constant level balloons. *Journal of Geophysical Research: Atmospheres*, *128*(4), e2022JD037585. doi: https://doi.org/10.1029/2022JD037585

Manzini, E., McFarlane, N. A., & McLandress, C. (1997). Impact of the doppler spread parameterization on the simulation of the middle atmosphere circulation using the ma/echam4 general circulation model. *Journal of Geophysical Research: Atmospheres*, *102*(D22), 25751-25762. doi: 10.1029/97JD01096

Orr, A., Bechtold, P., Scinocca, J., Ern, M., & Janiskova, M. (2010). Improved middle atmosphere climate and forecasts in the ecmwf model through a nonorographic gravity wave drag parameterization. *Journal of Climate*, *23*(22), 5905 - 5926. doi: https://doi.org/10.1175/2010JCLI3490.1

Plougonven, R., Jewtoukoff, V., de la Cámara, A., Lott, F., & Hertzog, A. (2017). On the relation between gravity waves and wind speed in the lower stratosphere over the southern ocean. *J. Atmos. Sci.*, *74*(4), 1075-1093. doi: 10.1175/JAS-D-16-0096.1

Rabier, F., Bouchard, A., Brun, E., Doerenbecher, A., Guedj, S., Guidard, V., ... Steinle, P. (2010, January). The Concordiasi Project in Antarctica. *Bulletin of the American Meteorological Society*, *91*(1), 69-86. Retrieved from `https://hal-insu.archives-ouvertes.fr/insu-00562459` doi: 10.1175/2009BAMS2764.1

Richter, J. H., Sassi, F., & Garcia, R. R. (2010). Toward a physically based gravity wave source parameterization in a general circulation model. *Journal of the Atmospheric Sciences*, *67*(1), 136 - 156. doi: 10.1175/2009JAS3112.1

Scaife, A. A., Butchart, N., Warner, C. D., & Swinbank, R. (2002). Impact of a spectral gravity wave parameterization on the stratosphere in the met office unified model. *Journal of the Atmospheric Sciences*, *59*(9), 1473 - 1489. doi: https://doi.org/10.1175/1520-0469(2002)059⟨1473:IOASGW⟩2.0.CO;2

Scinocca, J. F. (2003). An accurate spectral nonorographic gravity wave drag parameterization for general circulation models. *Journal of the Atmospheric Sciences*, *60*(4), 667 - 682. doi: https://doi.org/10.1175/1520-0469(2003)060⟨0667:AASNGW⟩2.0.CO;2

Serva, F., Cagnazzo, C., Riccio, A., & Manzini, E. (2018). Impact of a stochastic nonorographic gravity wave parameterization on the stratospheric dynamics of a general circulation model. *Journal of Advances in Modeling Earth Systems*, *10*(9), 2147-2162. doi: https://doi.org/10.1029/2018MS001297

Song, I.-S., & Chun, H.-Y. (2005). Momentum flux spectrum of convectively forced internal gravity waves and its application to gravity wave drag parameterization. part i: Theory. *J. Atmos. Sci.*, *62*(1), 107-124. doi: https://doi.org/10.1175/JAS-3363.1

Warner, C. D., & McIntyre, M. E. (1996). On the propagation and dissipation of gravity wave spectra through a realistic middle atmosphere. *J. Atmos. Sci.*, *53*(22), 3213-3235. doi: 10.1175/1520-0469(1996)053⟨3213:OTPADO⟩2.0.CO;2

Warner, C. D., & McIntyre, M. E. (1999). Toward an ultra-simple spectral gravity wave parameterization for general circulation models. *Earth, Planets and Space*, *51*, 475–484. doi: 10.1186/BF03353209

602

# Supplementary: Phase 1 flights and models

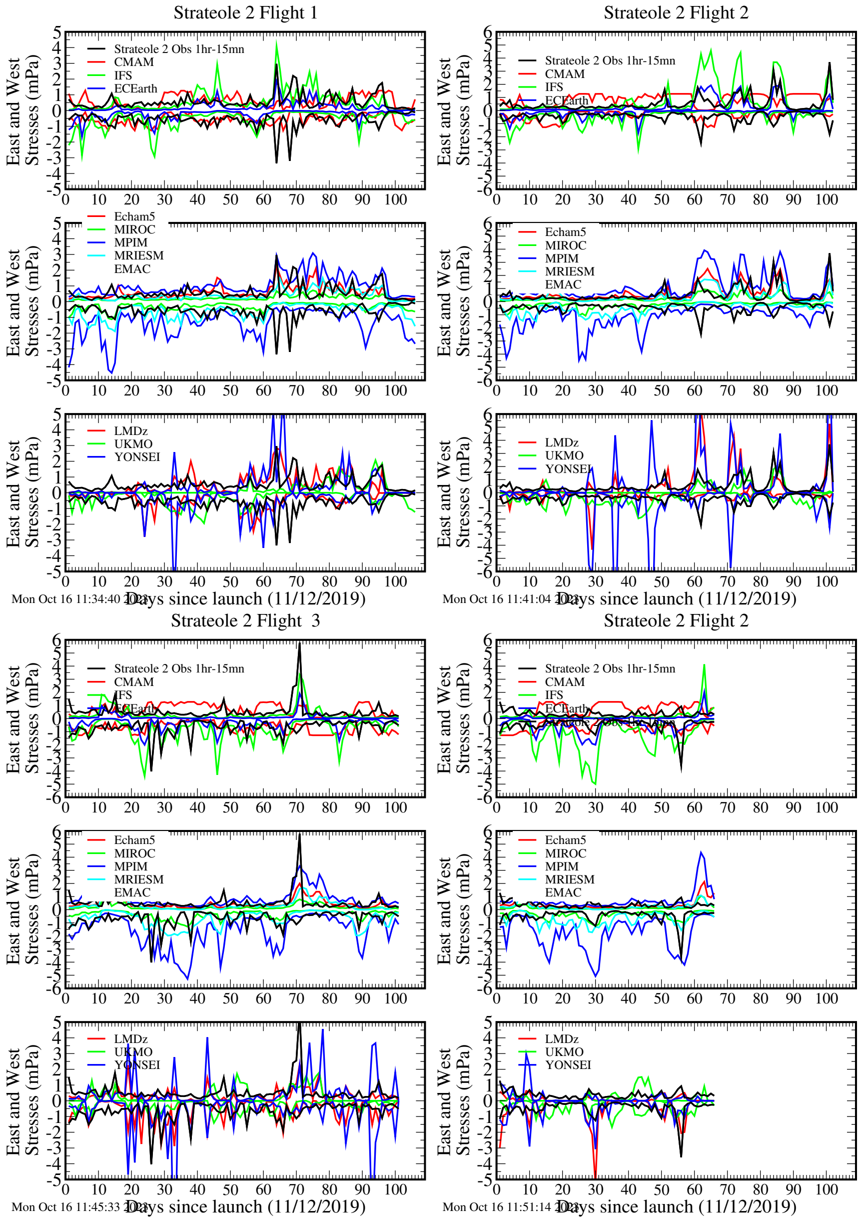

## Supplementary: Phase 1 flights and models (continued)

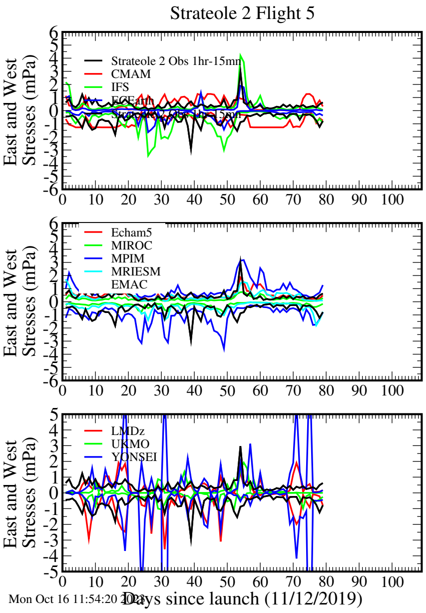


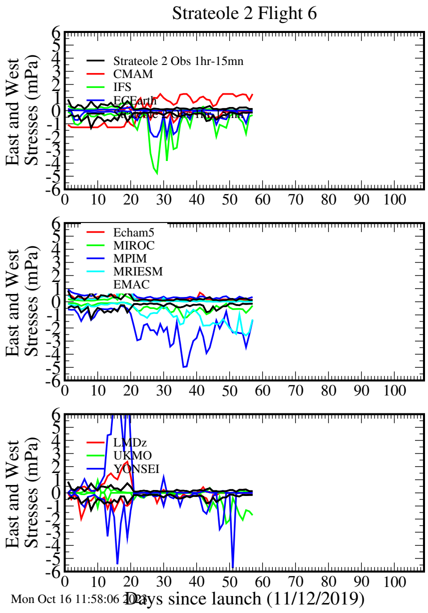


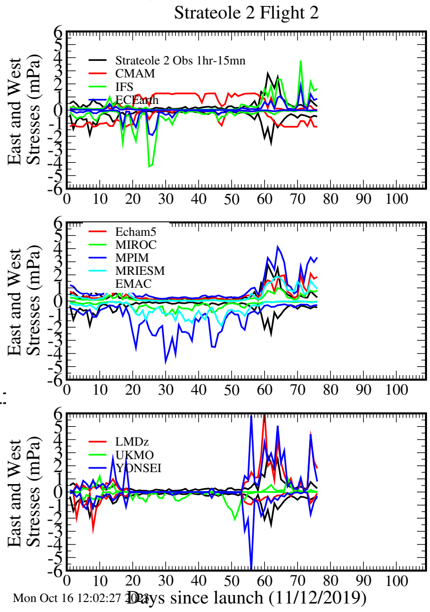


Figures/Balloon_7_East_West_1h

# Supplementary: Phase 2 flights and models

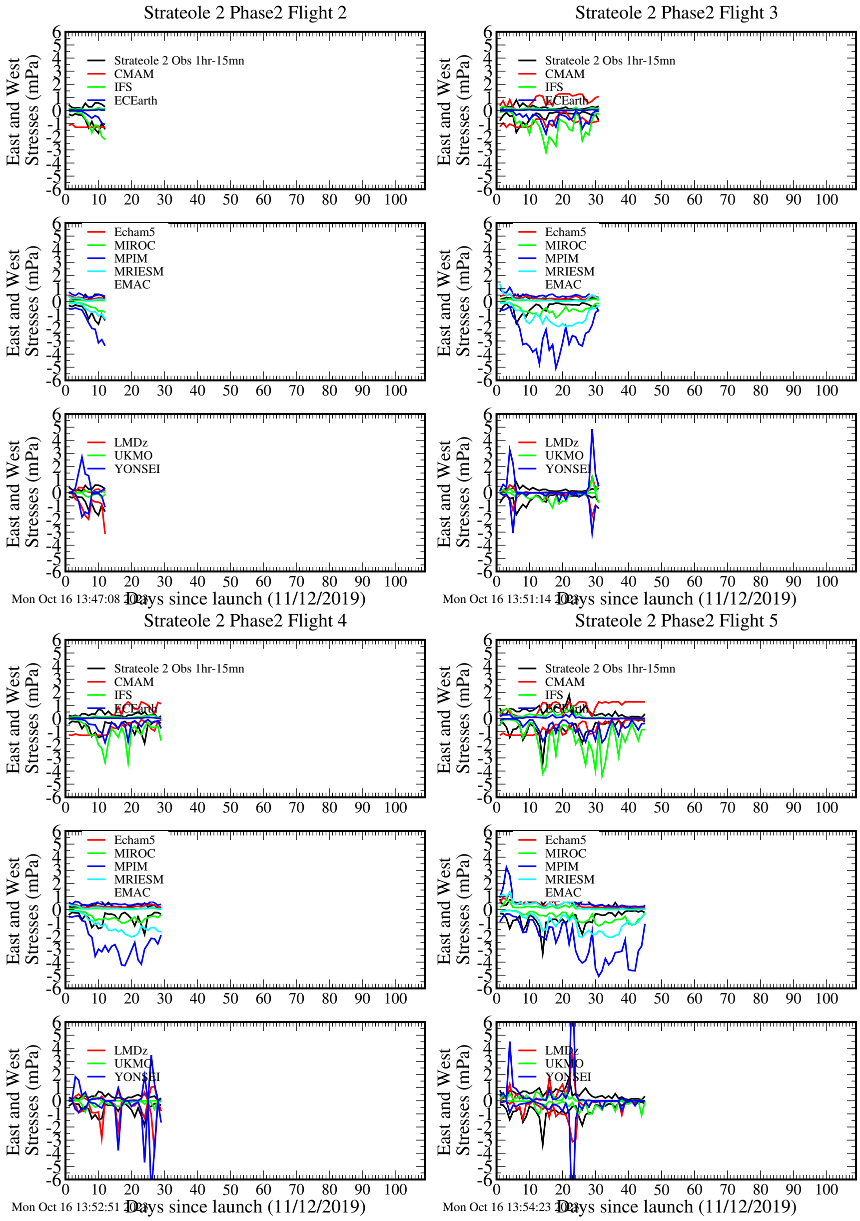

## Supplementary: Phase 2 flights and models (continued)

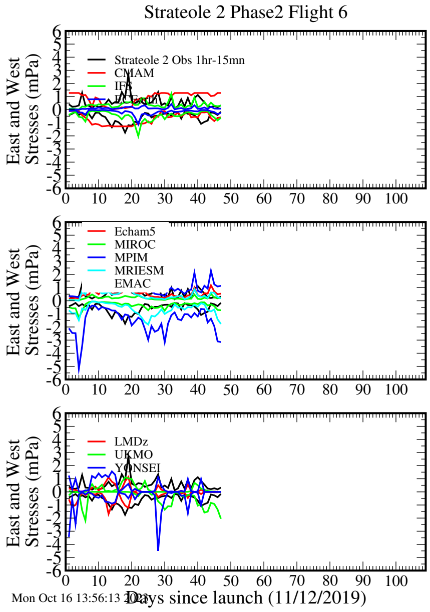


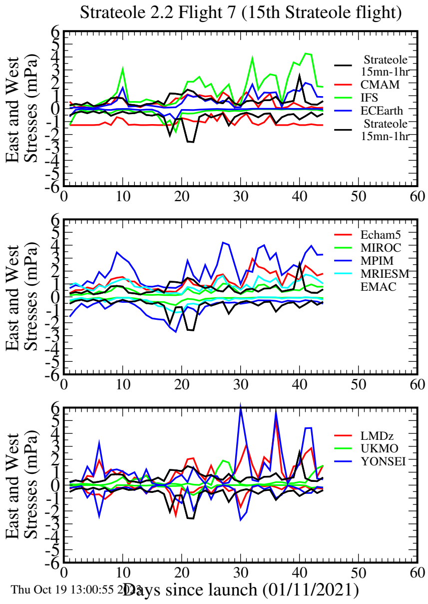


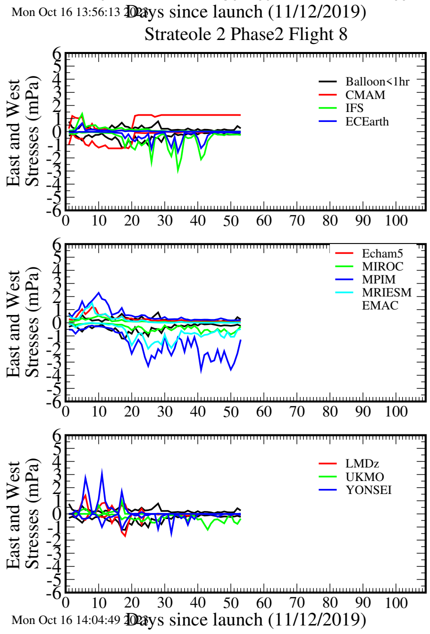


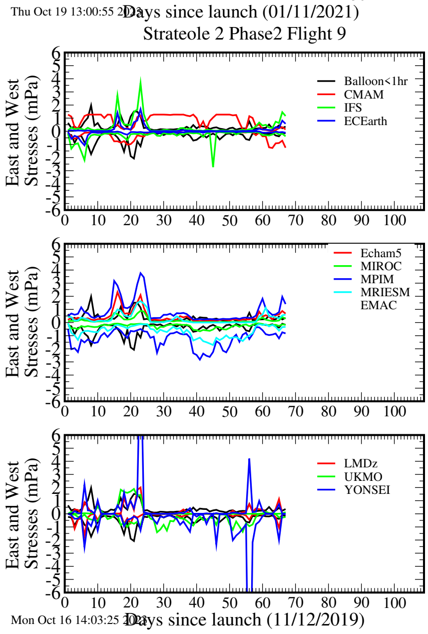

## Supplementary: Phase 2 flights and models (continued)

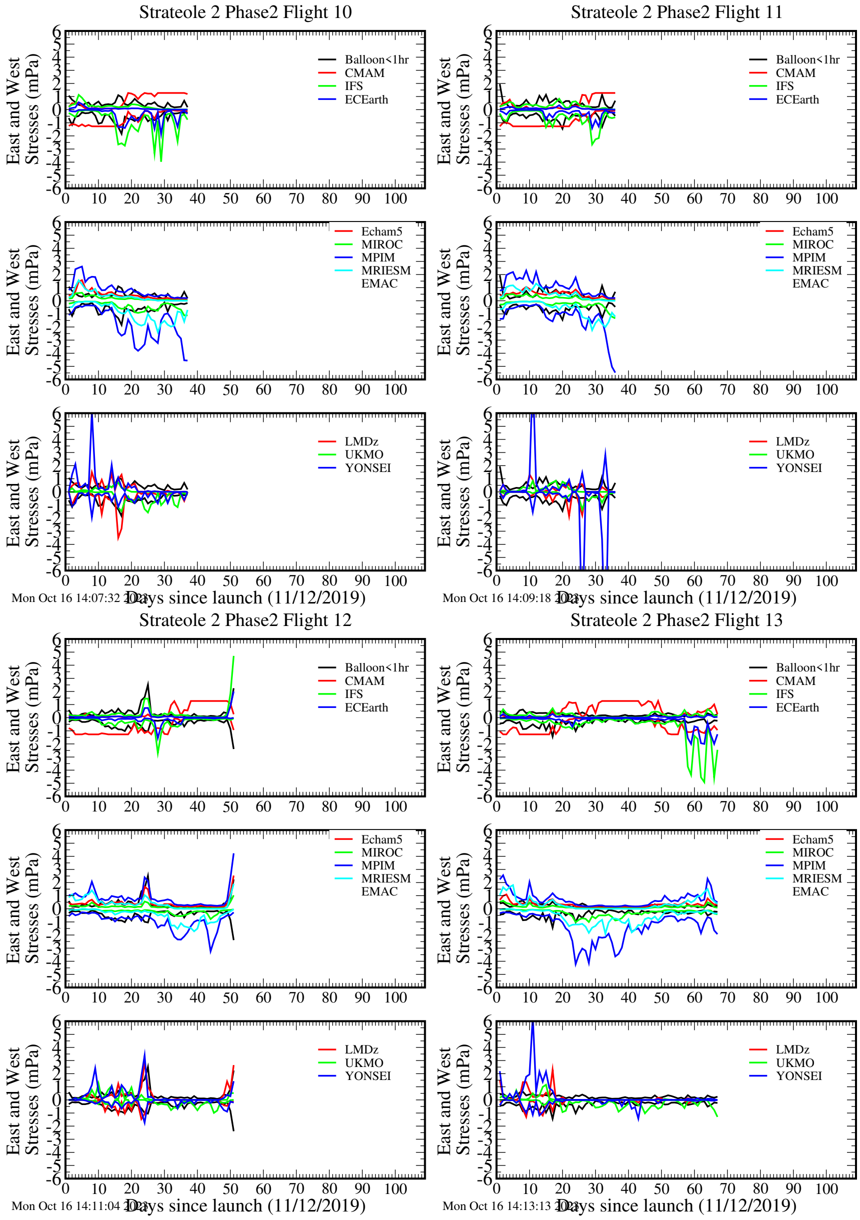


## Supplementary: Phase 2 flights and models (continued)

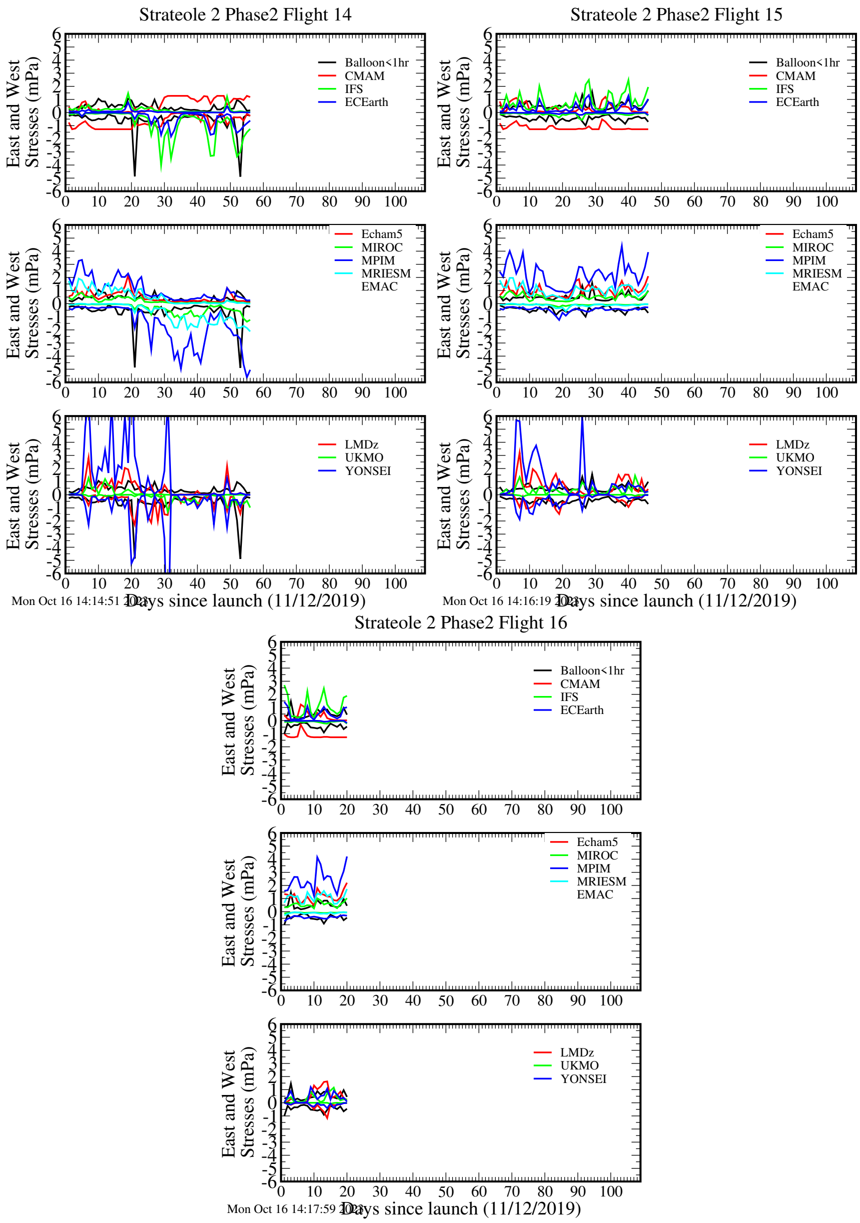
Strateole 2 Phase2 Flight 14
Strateole 2 Phase2 Flight 15
Strateole 2 Phase2 Flight 16
East and West Stresses (mPa)
Balloon<1hr
CMAM
IFS
ECEarth
Echam5
MIROC
MPIM
MRIESM
EMAC
LMDz
UKMO
YONSEI
Days since launch (11/12/2019)
Mon Oct 16 14:14:51 2023
Mon Oct 16 14:16:19 2023
Mon Oct 16 14:17:59 2023